

Linkage Isomerism in the Binding of Pentapeptide Ac-His(Ala)₃His-NH₂ to (Ethylenediamine)Palladium(II): Effect of the Binding Mode on Peptide ConformationHuy N. Hoang,^{†,‡} Gavin K. Bryant,[†] Michael J. Kelso,[‡] Renee L. Beyer,[‡] Trevor G. Appleton,^{*,†} and David P. Fairlie^{*,‡}

Centre for Metals in Biology, School of Molecular & Microbial Sciences, and Institute for Molecular Bioscience, The University of Queensland, Brisbane, Qld., Australia 4072

Received May 28, 2008

The reaction of the pentapeptide Ac-His1-Ala2-Ala3-Ala4-His5-NH₂ (AcHAAAHNH₂) (**1**) with [Pd(en)(ONO₂)₂] (en = NH₂CH₂CH₂NH₂) in either DMF-*d*⁷ or H₂O:D₂O (90%:10%) gave three linkage isomers of [Pd(en)(AcHAAAHNH₂)]²⁺ (**2**), **2a**, **2b**, and **2c**, which differ only in which pair of imidazole nitrogen atoms bind to Pd. In the most abundant isomer, **2a**, Pd is bound by N1 from each of the two imidazole rings. In the minor isomers **2b** and **2c**, Pd is bound by N1(His1) and N3(His5) and by N3(His1) and N1(His5), respectively. The reactions of [Pd(en)(ONO₂)₂] with the N-methylated peptides Ac-(N3-MeHis)-Ala-Ala-Ala-(N3-MeHis)-NH₂ (AcH[#]AAAH[#]NH₂) (**3**), Ac-(N3-MeHis)-Ala-Ala-Ala-(N1-MeHis)-NH₂ (AcH[#]AAAH[#]NH₂) (**4**), and Ac-(N1-MeHis)-Ala-Ala-Ala-(N3-MeHis)-NH₂ (AcH[#]AAAH[#]NH₂) (**5**) each gave a single species [Pd(en)(peptide)]²⁺ in N,N-dimethylformamide (DMF) or aqueous solution, **7**, **8**, and **9**, respectively, with Pd bound by the two nonmethylated imidazole nitrogen atoms in each case. These complexes were analogous to **2a**, **2b**, and **2c**, respectively. Ac-(N1-MeHis)-Ala-Ala-Ala-(N1-MeHis)-NH₂ (AcH[#]AAAH[#]NH₂) (**6**) with [Pd(en)(ONO₂)₂] in DMF slowly gave a single product, [Pd(en)(AcH[#]AAAH[#]NH₂)]²⁺ (**10**), in which Pd was bound by the N3 of each imidazole ring. The corresponding linkage isomer of **2** was not observed. Complex **10** was also the major product in aqueous solution, but other species were also present. All compounds were exhaustively characterized in solution by multinuclear 1D (¹H, ¹³C, and, with ¹⁵N-labeled ethylenediamine, ¹⁵N) and 2D (correlation spectroscopy, total correlation spectroscopy, transverse rotating-frame Overhauser effect spectroscopy (T-ROESY), heteronuclear multiple-bond correlation, and heteronuclear single quantum coherence) NMR spectra, circular dichroism (CD) spectra, electrospray mass spectroscopy, and reversed-phase high-performance liquid chromatography. ROESY spectra were used to calculate the structure of **2a**, which contained a single turn of a peptide α helix in both DMF and water, the helix being better defined in DMF. The Pd(en)²⁺ moiety was not used in structure calculations, but its location and coordination by one imidazole N1 from each histidine to form a 22-membered metallocycle were unambiguously established. Convergence of the structures was greatest when calculated with two hydrogen-bond constraints (Ala4 peptide NH...OC acetyl and His5 peptide NH...OC-His1) that were indicated by the low temperature dependence of these NH chemical shifts. Vicinal HN-CHα coupling constants and chemical shifts of α-H atoms were also consistent with a helical conformation. Similar long-range ROE correlations were observed for [Pd(en)(AcH[#]AAAH[#]NH₂)]²⁺ (**7**), which displayed a CD spectrum in aqueous solution that suggested the presence of some helicity. Long-range ROE correlations were not observed for **8**, **9**, or **10**, but a combination of NMR data and CD spectroscopy was interpreted in terms of the conformational behavior of the coordinated pentapeptide. Only for the linkage isomer [Pd(en)(AcH[#]AAAH[#]NH₂)]²⁺ (**8**) was there evidence of a contribution from a helical conformation. The data for **8** were interpreted as interconversion between the helix and random coil conformations. Zn²⁺ with peptides gave broad NMR peaks attributed to lability of this metal ion, while reactions of *cis*-[Pt(NH₃)₂(ONO₂)₂] were slow, giving a complex mixture of products rather than the macrochelate ring observed with Pd(en)²⁺. In summary, these studies indicate that Pd(en)²⁺ coordinates to histidine with similar preference for each of the two imidazole nitrogens, enabling the formation of up to four linkage isomers in its complexes with pentapeptides His-xxx-His. Only the N1–N1 linkage isomer that forms a 22-membered macrochelate ring is able to induce an α-helical peptide conformation, whereas the 20- and 21-membered rings of linkage isomers do not. This suggests that linkage isomeric mixtures may compromise histidine coordination to metal ions and reduce α-helicity.

Introduction

Short peptides (<15 residues) usually adopt random coil conformations in solution.^{1,2} If specific conformations such as

α helices could be stabilized for biologically relevant short peptides, they might be expected to show higher affinities and specificities for their targets, and may be more useful as biological probes and drug leads.³ When we commenced this work, methods used to stabilize helicity included the incorporation of unnatural amino acids;⁴ noncovalent side-chain con-

* Authors to whom correspondence should be addressed. E-mail: t.appleton@uq.edu.au (T.G.A.) or d.fairlie@imb.uq.edu.au (D.P.F.).

[†] Centre for Metals in Biology, School of Molecular & Microbial Sciences.

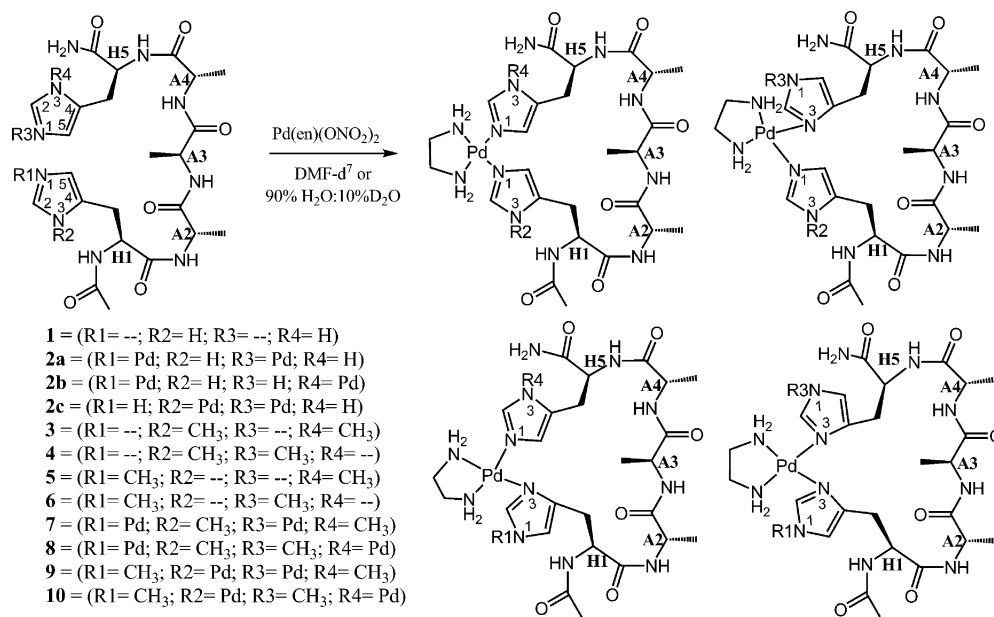
[‡] Institute for Molecular Bioscience.

(1) A preliminary communication of the structure in DMF alone has been made by us previously: Kelso, M. J.; Hoang, H. N.; Appleton, T. G.; Fairlie, D. P. *J. Am. Chem. Soc.* **2000**, *122*, 10488–10489.

(2) (a) Zimm, B.; Bragg, J. *J. Chem. Phys.* **1959**, *31*, 526–535. (b) Scholtz, A.; Baldwin, R. L. *Annu. Rev. Biophys. Biomol. Struct.* **1992**, *21*, 95–118.

(3) Fairlie, D.; West, M.; Wong, A. *Curr. Med. Chem.* **1998**, *5*, 29–62.

Scheme 1. Products of Reaction between HAAA (1) and $[\text{Pd}(\text{en})(\text{ONO}_2)_2]$, Showing Three $[\text{Pd}(\text{en})(\text{HAAA})]^{2+}$ Isomers and Methylated Complexes As Well As the Numbering Scheme for Imidazole



straints like salt bridges or hydrophobic interactions;⁵ covalent side-chain linkers such as disulfide, lactam, and hydrazone bridges;⁶ and templates that nucleate or cap helices.⁷ Oligomers of β and γ amino acids have also shown promise as helix mimetics.⁸ These methods were only successful when peptides were long enough to allow multiple turns of an α helix. Since then, our team has shown that pentapeptides can be stabilized in an α -helical turn by using a covalent lactam bridge between the side chains of lysine and aspartate five residues apart,^{6g,h} the only other stable single α -helical turn reported to date.

Metal ions such as Zn^{2+} , Cd^{2+} , and Ru^{2+} have been reported to stabilize helical conformations in oligopeptides when metal-coordinating histidines or cysteines were separated by three intervening residues (i and $i + 4$ positions).⁹

The conclusion about helicity was based on changes in circular dichroism (CD) spectra, usually for peptides with ≥ 15 residues or more, or under other conditions that favor α -helicity (e.g., 4 °C, salt, trifluoroethanol). There is still no compelling structural evidence (crystallographic or NMR) of helix induction in short peptides by metal ions.

Studies on peptides containing a single His residue have shown that metal ions tend to bind to an imidazole nitrogen atom of histidine first and subsequently bind to a deprotonated peptide nitrogen atom to form a small six-membered N₃N(peptide) chelate ring.¹⁰ Similar small chelate rings are formed when Cu(II) and Ni(II) bind to peptides containing two His residues.¹¹ Metal ions such as Pt(II)¹² and Pd(II)¹³ have a high affinity for imidazole nitrogens of histidines, but most reports involve only a single histidine. For reactions between Pt(dien)²⁺ (dien = diethylenetriamine), peptides containing neighboring histidine, and methionine residues, facile migration of the metal ion between binding sites has been observed.¹⁴

(4) (a) Rajashankar, K. R.; Ramakumar, S.; Jain, R. M.; Chauhan, V. S. *J. Am. Chem. Soc.* **1995**, *117*, 10129–10130. (b) Karle, I. L.; Balarum, P. *Biochemistry* **1990**, *29*, 6747–6761.

(5) (a) Mayne, L.; Englander, S. W.; Qui, R.; Yang, J.; Gong, Y.; Spek, E. J.; Kallenbach, N. R. *J. Am. Chem. Soc.* **1998**, *120*, 10643–10645. (b) Albert, J. S.; Hamilton, A. *Biochemistry* **1995**, *34*, 984–990.

(6) (a) Ravi, A.; Venkataram, B. V.; Balarum, P. *J. Am. Chem. Soc.* **1983**, *105*, 105–109. (b) Schievano, E.; Mammi, S.; Bisello, A.; Rosenblatt, M.; Chorev, M.; Peggion, E. *J. Pept. Sci.* **1999**, *5*, 330–337. (c) Bracken, C.; Gulyas, J.; Taylor, J. W.; Baum, J. *J. Am. Chem. Soc.* **1994**, *116*, 6431–6432. (d) Phelan, J. C.; Skelton, N. J.; Braisted, A. C.; McDowell, R. S. *J. Am. Chem. Soc.* **1997**, *119*, 455–460. (e) Taylor, J. W.; Yu, C. *Biorg. Med. Chem.* **1999**, *7*, 161–175. (f) Gabezas, E.; Satterthwait, A. C. *J. Am. Chem. Soc.* **1999**, *121*, 3862–3875. (g) Shepherd, N. E.; Abbenante, G.; Fairlie, D. P. *Angew. Chem., Int. Ed.* **2004**, *43*, 2687–2690. (h) Shepherd, N. E.; Hoang, H. N.; Abbenante, G.; Fairlie, D. P. *J. Am. Chem. Soc.* **2005**, *127*, 2974–2983.

(7) (a) Kemp, D.; Curran, T.; Boyd, J.; Allen, T. *J. Org. Chem.* **1991**, *56*, 6683–6697. (b) Muller, K.; Obrecht, D.; Knierzinger, A.; Stankovic, C.; Spiegler, C.; Bannwarth, W.; Trzeciak, A.; Englert, G.; Labhardt, A. M.; Schoenholzer, P. *Perspect. Med. Chem.* **1993**, 513–531. (c) Austin, R.; Maplestone, R. A.; Seffler, A. M.; Liu, K.; Hruzewicz, W. N.; Liu, C.; Cho, H. S.; Wemmer, D. E.; Bartlett, P. A. *J. Am. Chem. Soc.* **1997**, *119*, 6461–6472. (d) Aurora, R.; Rose, G. D. *Protein Sci.* **1998**, *7*, 21–38.

(8) (a) Stigers, K. D.; Soth, M. J.; Nowick, J. S. *Curr. Opin. Chem. Biol.* **1999**, *3*, 714. (b) Hanessian, S.; Luo, X.; Schaum, R. *Tetrahedron Lett.* **1999**, *40*, 4925. (c) Yang, D.; Qu, J.; Li, B.; Ng, F.-F.; Wang, X.-C.; Cheung, K.-K.; Wang, D.-P.; Wu, Y.-D. *J. Am. Chem. Soc.* **1999**, *121*, 589.

(9) (a) Ghadiri, M. R.; Choi, C. *J. Am. Chem. Soc.* **1990**, *112*, 1630–1632. (b) Ruan, F.; Chen, Y.; Hopkins, P. B. *J. Am. Chem. Soc.* **1990**, *112*, 9403–9404. (c) Ghadiri, M. R.; Fernholz, H. *J. Am. Chem. Soc.* **1990**, *112*, 9633–9635. (d) Kohn, W. D.; Sykes, B. D.; Hodges, R. S. *J. Am. Chem. Soc.* **1998**, *120*, 1124–1132.

(10) (a) Hahn, M.; Wolters, D.; Sheldrick, W. S.; Hulsbergen, F. B.; Reedijk, J. *JBIC* **1999**, *4*, 412. (b) Tsiveriotis, P.; Hadjiliadis, N.; Savropoulos, G. *Inorg. Chim. Acta* **1997**, *261*, 83. (c) Milinkovic, S. U.; Parac, T. N.; Djuran, M. I.; Kostic, N. M. *J. Chem. Soc., Dalton Trans.* **1997**, 2771. (d) Sovago, I. In *Biocoordination Chemistry, Coordination Equilibria in Biologically Active System* 1990, Ellis Horwood, London. (e) Tsiveriotis, P.; Hadjiliadis, N. *J. Chem. Soc., Dalton Trans.* **1999**, 459.

(11) Kozlowski, H.; Bal, W.; Dyba, M.; Kowalik-Jankowska, T. *Coord. Chem. Rev.* **1999**, *184*, 319.

(12) Appleton, T. G.; Pesch, F. J.; Wienken, M.; Menzer, S.; Lippert, B. *Inorg. Chem.* **1992**, *31*, 4410–4419.

(13) (a) Parac, T. N.; Kostic, N. M. *Inorg. Chem.* **1998**, *37*, 2141–2144. (b) Parac, T. N.; Ullman, G. M.; Kostic, N. M. *J. Am. Chem. Soc.* **1999**, *121*, 3127–3135.

(14) Hahn, M.; Wolters, D.; Sheldrick, W. S.; Hulsbergen, F. B.; Reedijk, J. *JBIC, J. Biol. Inorg. Chem.* **1999**, *4*, 412–420.

[Pt(en)(H₂O)₂]²⁺ and *cis*-[Pt(NH₃)₂(H₂O)₂]²⁺ have also been reacted with other peptides containing histidine and methionine residues, such as Ac-His-Ala-Ala-Ala-Met-OH.^{15,16} For Pt(en)²⁺ with this peptide,¹⁵ there was an initial formation of a six-membered chelate ring involving methionine sulfur and the adjacent peptide nitrogen atom, with subsequent slow isomerization to large chelate rings (“macrochelates”) involving methionine S and histidine imidazole (N1 or, less favorable, N3). Formation of the large chelate ring was found to be faster for this peptide with histidine and methionine at *i* and (*i* + 4) positions, and it was suggested that this might be due to the proximity of these side chains in an α helix, but there was no evidence for conformation of the peptide bound by Pt(en)²⁺. With this peptide, *cis*-Pt(NH₃)₂²⁺ also formed a six-membered chelate ring, but subsequent reactions involved amine loss and peptide cleavage rather than the formation of large chelate rings.¹⁶

Reactions have been described between [Pd(en)(H₂O)₂]²⁺ (en = ethylenediamine) and an oligopeptide containing histidines at positions 5 and 9.¹⁷ This peptide reportedly bound two Pd(en)²⁺ moieties, one histidine bound to each Pd through either N1 or N3 imidazole nitrogens. Tsiveriotis and Hadjiliadis¹⁷ studied reactions of *cis*-diammineplatinum(II) complexes with pentapeptides HXXXH, which were unprotected at both ends, and reportedly formed a six-membered chelate ring involving imidazole N3 (His1) and the terminal amine nitrogen atom. To our knowledge, there has never been a conclusive report of a metal ion binding to two histidine residues of an oligopeptide to form a large chelate ring, prior to our own work here.¹

On the other hand, metal ions are often found in metalloproteins bound to two or more histidine residues well-separated in sequence but brought together by folding of the protein (e.g., plastocyanin,¹⁸ thermolysin,¹⁹ and zinc finger proteins²⁰).

We now describe the formation of metallopeptides with imidazole nitrogen atoms of two histidine residues simultaneously coordinated to Pd(II) forming a large chelate ring. The reaction of pentapeptide Ac-His1-Ala2-Ala3-Ala4-His5-NH₂ (**1**) with [Pd(en)(ONO₂)₂] in N,N-dimethylformamide (DMF) or water (Scheme 1) produces three metallocycles (**2a**, **2b**, and **2c**). Our preliminary communication¹ showed that the predominant linkage isomer **2a** was a 22-membered macrocyclic metallopeptide with the peptide bound to metal through two histidine N1 atoms, and an NMR structural study demonstrated the first single α -helical turn in a pentapeptide, induced by metal binding. In the minor isomers, the peptide

was bound through N1(His1) and N3(His5) (**2b**), and through N3(His1) and N1(His5) (**2c**). These were not present in sufficiently high concentrations for reliable structural information to be obtained.

We have since studied reactions of Pd(en)²⁺ with small peptides containing histidines at *i* and *i* + 4 intervals.²¹ To simplify the chemistry, the possibility of linkage isomers was removed by using histidines in which N3 was methylated (N3MeHis, or H*), leaving only N1 for binding. This methylhistidine isomer was chosen because **2a** was the thermodynamically preferred isomer of [Pd(en)(AcHAAAH-NH₂)]²⁺, and because it had a stable α -helical peptide structure. There has not previously been any study of conformational behavior for the linkage isomers **2b** and **2c**. To address this issue, we also study here complexes formed by the reaction of Pd(en)²⁺ with peptides containing N3MeHis (H*) and N1MeHis (H[#]):



Experimental Section

General. Fmoc-Ala-OH and Fmoc-His(Trt)-OH (Novabiochem, Melbourne, Australia), Fmoc-N3-methyl-His-OH and Fmoc-N1-methyl-His-OH (Bachem AG, Switzerland), 2-(1H-benzotriazol-1-yl)-1,1,3,3-tetramethyluronium hexafluorophosphate, HBTU (Richelieu Biotechnologies, Quebec, Canada), and all other reagents of peptide synthesis grade (Auspep, Melbourne, Australia) were obtained commercially. Semipreparative high-performance liquid chromatography (HPLC) purifications were performed using a Waters Delta 600 chromatography system fitted with a Waters 486 tunable absorbance detector set at 254 nm. Electrospray mass spectra were recorded on a Finnigan Newstar 2001 FTMS with a 3 T magnet and Analytica API source. Circular dichroism measurements were performed using a Jasco model J-710 spectropolarimeter, which was routinely calibrated with (1S)-(+)-10-camphorsulfonic acid. Each metallopeptide complex was dissolved in water (50 μ M) at different pH values from 2 to 7. The temperature was controlled using a Neslab RTE-111 circulating water bath. Spectra were recorded at 298 K, with a 0.1 cm Jasco quartz cell over the wavelength range 260–185 at 50 nm/min, with a bandwidth of 1.0 nm, a response time of 2 s, a resolution step width of 0.1 nm, and sensitivity of 100 mM \cdot deg. Each spectrum represents the average of five scans with smoothing to reduce noise.

Synthesis and Characterization of Ac-HAAAH-NH₂ (1**) and N-Methylated Histidine Analogues.** Peptide **1** was prepared by manual stepwise solid-phase peptide synthesis using HBTU/diisopropylethylamine (DIPEA) activation for Fmoc chemistry²² on methylbenzhydrylamine (Novabiochem) resin (substitution 0.72 mmol \cdot g⁻¹, 0.25 mmol \cdot g scale, 350 mg of resin). Histidines were protected with trityl (Trt) groups during the peptide assembly. Four

(15) Wolters, D.; Sheldrick, W. S. *J. Chem. Soc., Dalton Trans.* **1999**, 1121–1129.

(16) Hahn, M.; Kleine, M.; Sheldrick, W. S. *J. Biol. Inorg. Chem.* **2001**, 556–566.

(17) Tsiveriotis, P.; Hadjiliadis, N. *J. Chem. Soc., Dalton Trans.* **1999**, 459–465.

(18) Xue, Y.; Okvist, M.; Hansson, O.; Young, S. *Protein Sci.* **1998**, 7, 2099.

(19) Holland, D. R.; Hausrath, A. C.; Juers, D.; Matthews, B. W. *Protein Sci.* **1995**, 4, 1955.

(20) (a) Greisman, H. A.; Pabo, C. O. *Science* **1997**, 275, 657. (b) Krizek, B. A.; Amann, B. T.; Kilfoil, V. J.; Merkle, D. L.; Berg, J. M. *J. Am. Chem. Soc.* **1991**, 113, 4518.

(21) (a) Kelso, M. J.; Hoang, H. N.; Oliver, W.; Sokolenko, N.; March, D. R.; Appleton, T. G.; Fairlie, D. P. *Angew. Chem., Int. Ed. Engl.* **2002**, 42, 421. (b) Beyer, R. L.; Hoang, H. N.; Appleton, T. G.; Fairlie, D. P. *J. Am. Chem. Soc.* **2004**, 126, 15096.

(22) Engelbretsen, D. R.; Garnham, B. G.; Bergman, D. A.; Alewood, P. F. *Tetrahedron Lett.* **1995**, 36, 8871.

equivalents of amino acid, 4 equiv of HBTU, and 2 equiv of DIPEA were employed in each coupling step (except for the coupling of Fmoc-N3-Me-His-OH, where only 2 equiv of amino acid and HBTU were used). Fmoc deprotections were achieved by 2 × 2 min treatments with 1:1 piperidine/DMF. Coupling yields were monitored by a quantitative ninhydrin assay,²³ and double couplings were employed for yields below 99.8%. N-terminal acetylation was achieved by treating the fully assembled peptide resin with a solution containing 870 μL of acetic anhydride, 470 μL of DIPEA, and DMF to 15 mL (2 × 5 min treatments). The peptide was cleaved from the resin and the Trt protecting groups simultaneously removed by treatment for 2 h with a solution containing 95% trifluoroacetic acid (TFA): 2.5% H₂O and 2.5% triisopropylsilane (TIPS; 25 mL solution per 1 g of peptide resin). The solution was then filtered and concentrated *in vacuo* and the peptide precipitated with ice-cold diethyl ether. The peptide precipitate was filtered, redissolved in 50% A/50% B, and lyophilized. The crude peptide was purified by rp-HPLC (Vydac C18 column, 300 Å, 22 × 250 mm, 254nm) using a gradient from 0% to 50% solvent B (90% CH₃CN, 9.9% H₂O, 0.1% TFA) in solvent A (99.9% H₂O, 0.1% TFA) over 60 min. Yield = 25%. (*R*_t = 11 min). MS: [obsd (M + H⁺), 547.2; calcd, 547.2].

The peptides containing N-methylated histidine residues, **3**, **4**, **5**, and **6** were prepared by analogous methods, using the corresponding Fmoc-methylHis-OH reagents.

Synthesis of [Pd(¹⁵NH₂CH₂CH₂¹⁵NH₂)(ONO₂)₂]. Ethylenediamine·2HCl, with nitrogen atoms highly ¹⁵N-enriched (>98%), was prepared by reacting enriched potassium phthalimide with ethyleneglycol bis-tosylate as described.²⁴ [Pd(¹⁵NH₂CH₂CH₂-¹⁵NH₂)Cl₂], freshly prepared from labeled ethylenediamine,²⁵ was converted to [Pd(¹⁵NCH₂CH₂¹⁵NH₂)(ONO₂)₂] as described.²⁶ *cis*-[Pt(¹⁵NH₃)₂(ONO₂)₂] was prepared as reported.²⁶

Metallopeptides 2, 7–10. Ac-HAAAH-NH₂ (**1**) (12 mg, 22 μmol) and [Pd(en)(ONO₂)₂] (6.4 mg, 22 μmol) were dissolved with stirring in 1 mL of DMF-*d*⁷ or water (90% H₂O, 10% D₂O) with the pH adjusted to 4.6 by adding NaOH or HNO₃. Similar procedures were used for reactions with peptides containing methylhistidines **3–6**.

NMR Spectroscopy. One-dimensional 500 MHz ¹H and 125.8 MHz ¹³C NMR spectra were obtained on a Bruker DRX-500 spectrometer. The 40.5 MHz ¹⁵N NMR spectra were obtained using a DEPT sequence on a Bruker AMX-400 spectrometer fitted with a 5 mm broad-band tunable probe. All spectra were recorded at 298 K. Spectra for DMF-*d*⁷ were locked on the CD₃ signal and those for water on the deuterium signal from 10% D₂O. ¹H NMR spectra were typically obtained with a sweep width of 5485 Hz, 32 scans, and 32 K data points, ¹³C spectra with a sweep width of 20 840 Hz, 24 000 scans, and 65 K data points. In DMF-*d*⁷, the residual solvent peak from the aldehyde proton (7.96 ppm) or carbon (162.7 ppm) was used as a reference. In water, 1,4-dioxane was reference for both ¹H (3.70 ppm) and ¹³C (67.73 ppm) NMR spectra. ¹⁵N chemical shifts were referenced to ¹⁵NH₄⁺ (0.0 ppm) from 5 M (¹⁵NH₄)₂SO₄ in 1 M H₂SO₄, in a coaxial capillary. ¹³C and ¹⁵N NMR spectra were ¹H-decoupled.

Two-dimensional spectra were obtained at 298 K on a Bruker DRX-500 spectrometer. Correlation spectroscopy (COSY)²⁷ spectra were obtained using the standard Bruker pulse program cosydfrpt with 512 t1 increments in F1 and 2 K data points in F2 with 32 scans per increment. Total correlation spectroscopy (TOCSY)²⁸ spectra were obtained using pulse program MLEV-17 with an 80 ms mixing time, 350 F1 increments (16 scans each), and 2 K data points in F2. Transverse rotating-frame Overhauser effect spectroscopy (T-ROESY)²⁹ spectra were obtained using cw spin-lock (3 KHz (16.5 dB)) with a mixing time of 250 ms. A total of 600 increments were acquired in F1 with 2 K data points in F2 with 48 scans per increment. Heteronuclear single quantum coherence (HSQC)³⁰ spectra were obtained with 900 increments in F1, 2 K data points in F2, and 32 scans per increment. Heteronuclear multiple-bond correlation (HMBC) spectra were obtained with 1024 increments in F1, 2 K data points in F2, and 32 scans per increment. For ¹H NMR spectra in aqueous solution, solvent suppression was achieved using low-power presaturation during the relaxation delay or by using a 3–9–19 pulse sequence with gradients.³¹ Variable-temperature ¹H NMR spectra were recorded over the range 288–318 K.

Solution Structure for [Pd(en)(peptide)]²⁺ (2a**).** Intensities of ROE cross-peaks from the T-ROESY experiment were classified as strong (internuclear distance restraint ≤ 2.5 Å), medium (≤ 3.5 Å), weak (≤ 5.0 Å), or very weak (≤ 6.0 Å). A total of 44 such ROE distance restraints and three ³J_{NHCH α} (dihedral angle $\phi = -60 \pm 25^\circ$) coupling constant restraints were used initially to calculate 14 structures (ignoring Pd(en)²⁺) in a DMF solution, using a dynamic simulated annealing and energy minimization protocol in XPLOR (version 3.851)³² and refinement using the conjugate gradient Powell algorithm with 4000 cycles of energy minimization and a refined forcefield based on CHARMM.³² Backbone dihedral angle restraints were inferred from ³J_{NHCH α} coupling constants, with ϕ restrained to $-65 \pm 25^\circ$ for ³J_{NHCH α} ≤ 6 Hz. Peptide bond ω angles were all set to trans. Resulting structures, calculated without explicit hydrogen-bond restraints, showed reasonable convergence but with a number of small ROE violations. When Ala4 and His5 amide-NH protons were constrained by 5 → 1 α -helical hydrogen bonds to the acetyl and His1 carbonyl O atoms, respectively, the ROE violations disappeared, structural convergence improved, and energies for calculated structures markedly reduced. In water, the peptide hydrogen bonding was disrupted to some extent by water molecules, giving a less well-defined structure than in DMF. Structures were displayed using Insight II (v.2000, Molecular Simulations Inc., San Diego, CA).

(27) Derome, A.; Williamson, M. *J. Magn. Reson.* **1990**, *88*, 177–185.

(28) Bax, A.; Davis, D. G. *J. Magn. Reson.* **1985**, *65*, 355–360.

(29) (a) Bax, A.; Davis, D. G. *J. Magn. Reson.* **1985**, *65*, 355–360. (b) Hwang, T. L.; Shaka, A. J. *J. Chem. Soc.* **1992**, *114*, 3157–3159.

(30) (a) Palmer, A. G., III; Cavanagh, J.; Wright, P. E.; Rance, M. *J. Magn. Reson.* **1991**, *93*, 151–170. (b) Kay, L. E.; Keifer, P.; Saarinen, T. *J. Am. Chem. Soc.* **1992**, *114*, 10663–5. (c) Schleucher, J.; Schwendinger, M.; Satter, M.; Schmidt, P.; Schedletsky, O.; Glaser, S. J.; Sorensen, O. W.; Griesinger, C. *J. Biomol. NMR* **1994**, 301–306.

(31) (a) Piotto, M.; Saudek, V.; Sklenar, V. *J. Biomol. NMR* **1992**, 661–666. (b) Skenar, V.; Piotto, M.; Leppik, R.; Saudek, V. *J. Magn. Reson.* **1993**, *120*, 241–245.

(32) (a) Brünger, A. T. *X-PLOR Manual*, version 3.1; Yale University: New Haven, CT, 1992. (b) Nilges, M.; Gronenborn, A. M.; Brünger, A. T.; Clore, G. M. *Protein Eng.* **1988**, *2*, 27–38. (c) Brooks, B. R.; Brucoleri, R. E.; Olafson, B. D.; States, D. J.; Swaminathan, S.; Karplus, M. *J. Comput. Chem.* **1983**, *4*, 187–217.

(33) Wüthrich, K.; Billeter, M.; Braun, W. *J. Mol. Biol.* **1984**, *180*, 717–740.

(34) Wüthrich, K. *NMR of proteins and nucleic acids*; Wiley: New York, 1986.

(35) Karplus, M. *J. Am. Chem. Soc.* **1963**, *85*, 2870.

(23) Sarin, V.; Kent, S. B. H.; Tan, J. P.; Merrifield, R. B. *Anal. Biochem.* **1981**, *117*, 147.

(24) Appleton, T. G.; Bailey, A. J.; Bedgood, D. R., Jr.; Hall, J. R. *Inorg. Chem.* **1994**, *33*, 217.

(25) McCormack, J. B.; Jaynes, E. N.; Kaplan, R. I. *Inorg. Synth.* **1972**, *13*, 216.

(26) Appleton, T. G.; Berry, R. D.; Davis, C. A.; Hall, J. R.; Kimlin, H. A. *Inorg. Chem.* **1984**, *23*, 3514.

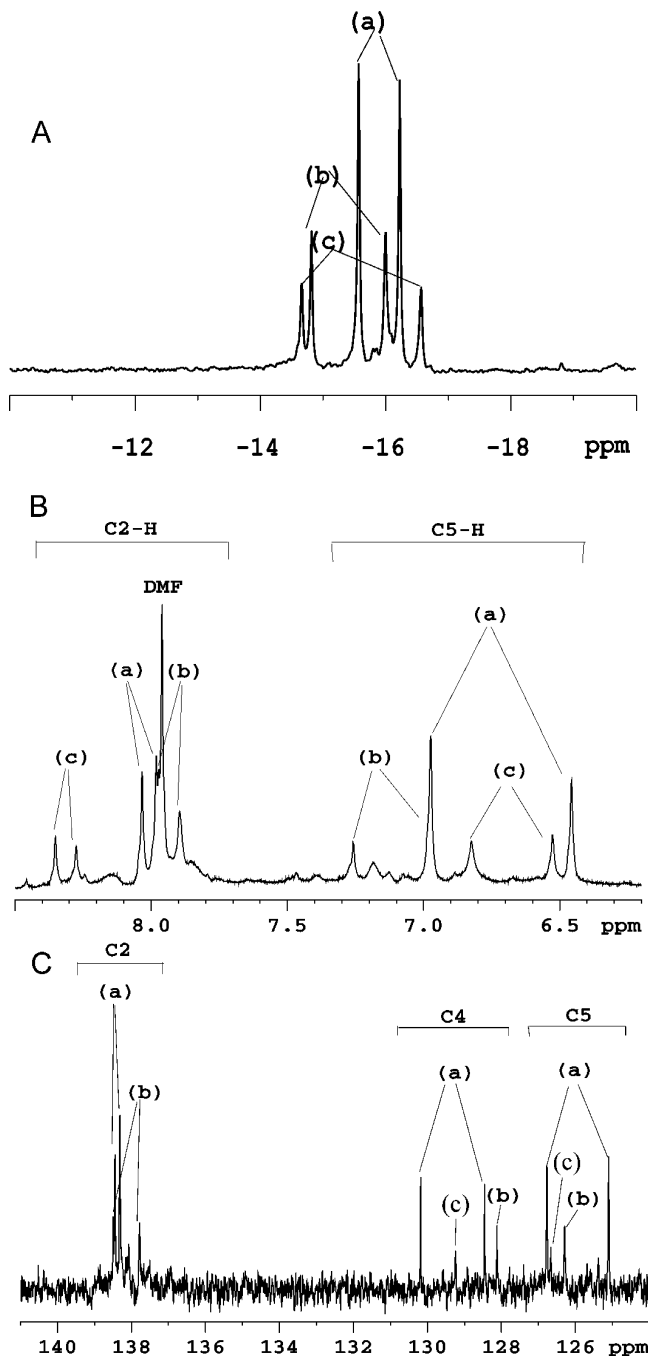


Figure 1. Multinuclear NMR spectra for the reaction between HAAAHAH (**1**) and $[\text{Pd}(\text{en}-^{15}\text{N})(\text{ONO}_2)_2]$, ratio 1:1, in $\text{DMF}-d_7$. (A) 40.5 MHz ^{15}N NMR spectrum showing three products of $[\text{Pd}(^{15}\text{en})(\text{HAAAHAH})]^{2+}$, **2a–c** (ratio 2:1:0.7). (B) Imidazole region of 500 MHz ^1H NMR spectrum with D_2O added to exchange all N–H proton signals, leaving only imidazole C–H signals (a, b, c) for clarity. (C) 125.8 MHz ^{13}C NMR spectrum (imidazole region only) showing chemical shifts for **2a**, **2b**, and **2c**.

Results

Peptides. Assignments of ^1H NMR resonances to residues of pentapeptide **1**, Ac-HAAAHAH-NH₂, were made using combined 1-D ^1H NMR and 2-D COSY, TOCSY, and T-ROESY NMR spectral data. The ^{13}C NMR assignments were made by 1-D ^{13}C and 2-D HSQC and HMBC spectra. The HSQC spectrum was used to obtain the one-bond correlation $^1J_{\text{CH}}$ and the HMBC spectrum to obtain the longer-range $^nJ_{\text{CH}}$. These techniques allowed assignment of

the imidazole and carbonyl C atoms. Assignments for all protons and carbon atoms in $\text{DMF}-d_7$ are given later. There were no unassigned signals, consistent with peptide **1** being the only species in solution. Chemical shifts for protons and carbon atoms of the pentapeptide in water were similar to those in $\text{DMF}-d_7$. Similar methods were used to assign peaks for peptides containing N-methylated histidines, **3–6** (Table S1, Supporting Information).

T-ROESY spectra for each peptide in both $\text{DMF}-d_7$ (for **1**, Figure S1, Supporting Information) and water (not shown) exhibited ROE correlations only for sequential amino acids along the peptide chain. There were no ROE cross peaks for a specific peptide conformation, so the free peptide is unstructured in both DMF and water, adopting only random coils.

Reaction of $[\text{Pd}(\text{en})(\text{ONO}_2)_2]$ with Ac-HAAAHAH-NH₂ (1**).** $[\text{Pd}(\text{en})(\text{ONO}_2)_2]$ is relatively labile with nitrate ligands being readily substituted in water to form $[\text{Pd}(\text{en})(\text{OH}_2)_2]^{2+}$,²⁴ the protonation state of the aqua ligand being pH-dependent. ^{15}N NMR spectra revealed a detectable equilibrium in DMF between $[\text{Pd}(\text{en})(\text{ONO}_2)_2]$, $[\text{Pd}(\text{en})(\text{ONO}_2)(\text{DMF}-O)]^+$, and $[\text{Pd}(\text{en})(\text{DMF}-O)_2]^{2+}$ (Table S2, Supporting Information). When $[\text{Pd}(^{15}\text{NH}_2\text{CH}_2\text{CH}_2^{15}\text{NH}_2)(\text{ONO}_2)_2]$ and peptide **1** were dissolved in water, the electrospray mass spectrum (Supporting Information Figure S2) revealed three sets of peaks, each with an isotope pattern characteristic for the presence of Pd. The most intense signal (corresponding to ^{106}Pd) within each peak was *m/e* 357.2, 713.4, and 827.4, corresponding respectively to $[\text{Pd}(\text{en})(\text{peptide})]^{2+}$, $[\text{Pd}(\text{en})(\text{peptide}-\text{H})]^+$, and $[\text{Pd}(\text{en})(\text{peptide})](\text{CF}_3\text{CO}_2)^+$. Traces of trifluoroacetic acid originate from the rpHPLC purification of the peptide and mass spectra are notoriously sensitive to this. The results are consistent with the presence in aqueous solution of a 1:1 palladium/peptide mononuclear complex, $[\text{Pd}(\text{en})(\text{Ac-HAAAHAH-NH}_2)]^{2+}$ (**2**), and this conclusion is supported by NMR data below.

The ^{15}N NMR spectrum (Figure 1a) for the peptide mixed with the palladium complex in $\text{DMF}-d_7$ showed three pairs of singlets (**2a/2b/2c**, intensity ratio 2:1:0.7), each pair due to an asymmetric ethylenediamine ligand of the metal complexes. Their chemical shifts (Table S2, Supporting Information) were all to lower field of a complex containing O-donor ligands, in a region ($\delta_{\text{N}} \sim 14.6$ to ~ 16.6) corresponding to ethylenediamine ^{15}N trans to a nitrogen-donor ligand (e.g., a histidine nitrogen).^{26,36} No peaks remained in solution from complexes with O-donor ligands.

In water, the ^1H -decoupled ^{15}N NMR spectrum (Figure S3, Supporting Information) showed three similar pairs of singlets, with slightly different intensity ratios, 2:1.5:1, similarly assigned to the three linkage isomers **2a**, **2b**, and **2c**. Chemical shifts are given in Table S2 (Supporting Information).

Three sets of peaks ($\sim 2:1:1$) were observed in both ^1H and ^{13}C NMR spectra (Figure 1b,c) and in 2-D NMR spectra (TOCSY, T-ROESY, HMBC, and HSQC), corresponding to linkage isomers **2a**, **2b**, and **2c** in both $\text{DMF}-d_7$ and water.

(36) Appleton, T. G.; Bailey, A. J.; Bedgood, D. R., Jr.; Hall, J. R. *Inorg. Chem.* **1994**, *33*, 3834.

Table 1. Deviations of C2, C4, and C5 Imidazole Chemical Shifts for Isomers **2a**, **2b**, and **2c** Relative to the Free Peptide **1**, $\Delta\delta = \delta_{Cn}(\mathbf{2a}$ or $\mathbf{2b}$ or $\mathbf{2c}) - \delta_{Cn}(\mathbf{1})$ in DMF- d^7 ($n = 2, 4,$ and 5)

complexes	$\Delta\delta^{13}\text{C}_{\text{imidazole}}$					
	$\Delta\delta_{C2}$		$\Delta\delta_{C4}$		$\Delta\delta_{C5}$	
	His1	His5	His1	His5	His1	His5
[Pd(en)(HAAA-H-N1,N1)] ²⁺ (2a)	3.55	3.56	-2.61	-0.72	8.57	6.97
[Pd(en)(HAAA-H-N1,N3)] ²⁺ (2b)	2.86	3.67	-2.92	8.07	8.00	-3.13
[Pd(en)(HAAA-H-N3,N1)] ²⁺ (2c)	3.44	3.36	5.98	-1.55	-0.70	8.57

Peaks in ¹H and ¹³C spectra were assigned using similar methods to those for free peptides. Chemical shifts in DMF- d^7 and water are given in Table S3 (Supporting Information). All expected resonances were observed and unambiguously assigned for the major linkage isomer **2a**, and most peaks were detectable and assigned for minor isomers **2b** and **2c**, except for just six of the 88 ¹H or ¹³C peaks shown in Table S2 (Supporting Information) that could not be unequivocally assigned due to spectral overlap. Each imidazole proton and carbon resonance from free peptide was significantly shifted after palladium addition, ¹H resonances tending to shift to a lower field while most ¹³C resonances shifted to higher field (Table S3, Supporting Information), consistent with both histidines coordinated via imidazole to Pd(II) in each metalloprotein. ¹H NMR signals were observed in each case for all five protons bound to backbone peptide N atoms, so no deprotonated peptide N atoms were bound to Pd. Expected peaks from amide and ethylenediamine NH₂ groups were also observed.

The 500 MHz T-ROESY spectra for peptide **1** and the products (**2a** and **2b** only, peaks from **2c** were undetectable) from the reaction with [Pd(en)(ONO₂)₂] in DMF- d^7 are given in Figure S2 (Supporting Information). ROE correlations were observed between protons of His1 and His5 imidazole rings for **2a**, indicating that they are in close proximity. Thus, two imidazole rings from one peptide are bound to one palladium in **2a** that must contain a large chelate ring with 22 ring atoms, rather than Pd²⁺ bridging between imidazole rings from two different peptide molecules. For **2a**, ROE correlations were also observed between amine protons on ethylenediamine and H2 protons on the imidazole rings, indicating that the Pd(ethylenediamine) chelate ring remained intact, leaving two coordination sites for binding to the peptide.

Linkage isomerism involving histidine bound to metal ions through imidazole N1 or N3 is well-established in the literature, and ¹³C chemical shifts for imidazole carbons are particularly diagnostic of each possible isomer.^{12,13} Binding to palladium through N1 would be expected to affect the chemical shifts of both C2 and C5, while binding through N3 should affect chemical shifts of C2 and C4. Table 1 illustrates such trends as differences between δ_C for each imidazole-C atom of **2a–2c** compared with free peptide **1**. There is a modest increase for δ_{C2} for each imidazole ring in each isomer. For isomer **2a**, there is a large increase in δ_{C5} for each imidazole ring and small decreases in δ_{C4} , consistent with N1 of each imidazole ring bound to palladium forming a 22-membered chelate ring (structure **2a** above). For isomer **2b**, there is a large increase in δ_{C4} for the imidazole ring of His5, and a large increase in δ_{C5} for the

imidazole ring of His1, indicating that N1 of His1 and N3 of His5 bind to palladium to form a 21-membered chelate ring (structure **2b** above). For isomer **2c**, there is a large increase in δ_{C4} for the imidazole ring of His1 and in δ_{C5} for the imidazole ring of His5, indicating that N3 of His1 and N1 of His5 bind to palladium (structure **2c** above). The fourth possible linkage isomer, with palladium bound by the two N3 atoms to form the smaller 20-membered chelate ring, was not observed presumably because of increased strain relative to the 21- and 22-membered rings of the other isomers.

Reactions of [Pd(en)(ONO₂)₂] with N-Methylhistidine Peptides. Proposed linkage isomers for the three sets of peaks in NMR spectra for [Pd(en)(AcHAAAHNH₂)] were supported by results for complexes of peptides methylated at one imidazole N. N-methylation prevents nitrogen coordination to metal, so that any coordination through histidine imidazole must be through the nonmethylated N. When [Pd(en)(ONO₂)₂] (with ¹⁵N enrichment) in DMF- d^7 or water was mixed with AcH*AAA*H*NH₂ (**3**) or AcH*AAA*H*NH₂ (**4**) or AcH#AAA*H*NH₂ (**5**), the ¹H-decoupled ¹⁵N NMR spectrum immediately after mixing showed two singlets of equal intensity in the range $\delta_N \sim 14.6–16.6$, as expected if in each case a single product was formed. Product **7** has the peptide bound through two N1's, corresponding to **2a**; in **8**, the peptide binds through N1 and N3, corresponding to **2b**, and **9** has the peptide bound through N3 and N1, corresponding to **2c**. Electrospray mass spectra of aqueous solutions were in accord with the presence of a single species [Pd(en)(peptide)]²⁺ in solution. ¹⁵N chemical shifts for these species are given in Table S2 (Supporting Information).

¹H or ¹³C NMR spectra for reactions in DMF- d^7 or water between [Pd(en)(ONO₂)₂] with peptides **3–5** in each case gave a single set of peaks corresponding to complexes **7–9**, respectively (Table S4, Supporting Information). Apart from the expected presence of additional singlets from N-methyl groups, the spectra of each species **7–9** were very similar to those of the corresponding isomers **2a**, **2b**, and **2c**, respectively, including the chemical shifts of imidazole carbon atoms. As with the isomers of **2**, all five protons bound to peptide N atoms gave signals, and ROE crosspeaks were observed between protons on the two histidine imidazole rings, and between these protons and ethylenediamine amine protons, as expected for a macrochelate ring involving binding of two histidine imidazole groups to a single Pd atom.

With peptide AcH#AAA*H*NH₂ (**6**), the ¹⁵N NMR spectrum showed the very slow formation of a single species (two singlets) in DMF- d^7 . The reaction was incomplete after 2 days. This product is a compound in which peptide was

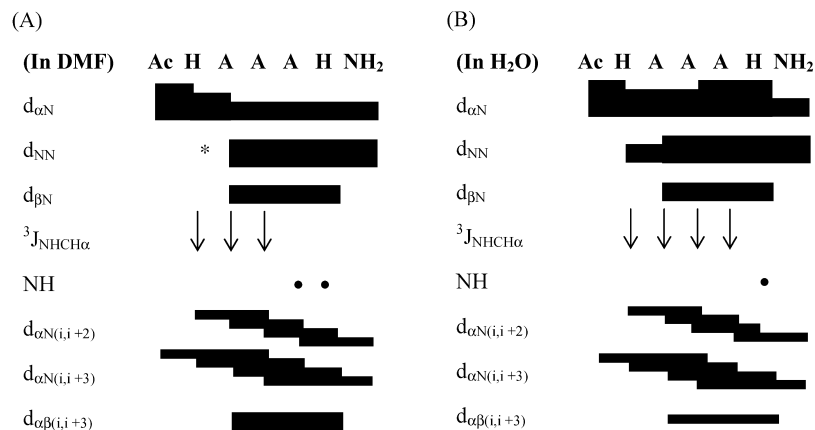


Figure 2. Summary of sequential and medium-range ROEs of $[\text{Pd}^{(15\text{en})}(\text{HAAAHH})]^{2+}$, isomer **2a** in (A) $\text{DMF-}d^7$, (B) 90% $\text{H}_2\text{O}/10\%$ D_2O . ROE intensities were classified as strong (upper distance constraint 2.5 Å), medium (3.5 Å), weak (5.0 Å), and very weak (6.0 Å) and are proportional to bar thickness. $^3J_{\text{NHCH}\alpha}$ coupling constants < 6 Hz are indicated by ↓. Amide NH's for which chemical shifts changed by < 3 ppb/K are indicated by •. The asterisk represents a ROE missing due to its proximity to the diagonal.

bound to two histidine N3 atoms in a 20-membered chelate ring (**10**). The corresponding linkage isomer was not observed for $[\text{Pd}(\text{en})(\text{AcHAAAHH}_2)]$ (**2**). The ^1H NMR spectrum of **10** in $\text{DMF-}d^7$ showed very broad peaks for the peptide NH, making a study of ROE crosspeaks for **10** very difficult, as their intensities were low (Table S4, Supporting Information). A determination of coupling constants and long- and medium-range ROEs was also not possible. In water, more than one product was formed. There was a strong peak at -16.16 ppm, and weaker signals at -16.52 and -17.04 ppm. There was also a strong peak at -19.95 ppm from $[\text{Pd}(\text{en})_2]^{2+}$ and at -27.39 ppm from $[\text{Pd}(\text{en})(\text{H}_2\text{O})_2]^{2+}$. In this case, there was clearly not a simple formation of a macrochelate ring, as in DMF.

Structure of $[\text{Pd}(\text{en})(\text{AcHAAAHH}_2-\text{NI},\text{NI})]^{2+}$ (2a**) in $\text{DMF-}d^7$.** T-ROESY NMR spectra for **2a** (Figure S4, Supporting Information) showed numerous ROE correlations. Those relevant to the three-dimensional structure are summarized in Figure 2 along with other key structural information for **2a**. Observed correlations for i to $i + 3$ and i to $i + 4$ residues that are especially characteristic of an α helix were the $\alpha\beta$ ($i, i + 3$) and αHN ($i, i + 3$) correlations between residues 1 and 4 and 2 and 5 within Ac-His1-Ala2-Ala3-Ala4-His5-NH₂ bound to Pd(II). Sequential amide HN–NH cross-peaks were observed with intensities ranging from medium to strong (Figure 2a), consistent with HN–NH distances < 3.0 Å, as required for a regular α helix.³³ Each of the $^3J_{\text{HNCH}\alpha}$ values for residues 1, 2, and 3 was less than 6 Hz, consistent with a helical structure for the peptide backbone^{34,35} (Figure 2a).

The upfield shift of ^1H NMR resonances for $\text{CH}\alpha$ of a peptide backbone is also usually a characteristic feature of induction of α helicity in a peptide.^{37,38} Figure 3A demonstrates that all five $\text{CH}\alpha$ signals for the peptide backbone in **2a** were indeed shifted upfield to various extents relative to their values for the free peptide **1**.

The temperature dependence for each of the amide NH ^1H NMR chemical shifts for **2a** is shown in Figure S5

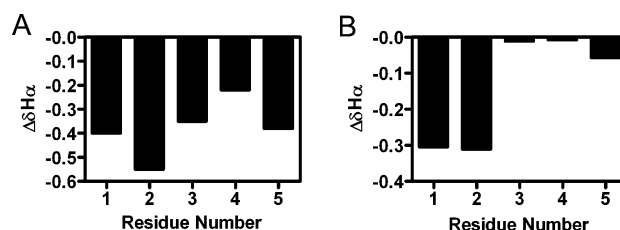


Figure 3. Deviations of $\text{CH}\alpha$ chemical shifts in $[\text{Pd}^{(15\text{en})}(\text{HAAAHH})]^{2+}$, isomer **2a** relative to the free peptide **1**, $\Delta\delta = \delta\text{CH}\alpha(\mathbf{2a}) - \delta\text{CH}\alpha(\mathbf{1})$ in (A) $\text{DMF-}d^7$ or (B) 90% $\text{H}_2\text{O}/10\%$ D_2O . Negative values indicate upfield shifts for **2a** versus **1** and are typical of α -helicity.

(Supporting Information). The temperature coefficient ($\Delta\delta_{\text{H}}/T$) for two of these amide protons (Ala4 and His5) was ≤ 3 ppb/deg, consistent with each being involved in a hydrogen bond.^{39,40} Chemical shifts for all of the other amide protons were much more sensitive to the temperature. Further evidence for the two hydrogen bonds comes from a deuterium exchange experiment in which a drop of D_2O was added to the $\text{DMF-}d^7$ solution. The same two amide NH protons exchanged with deuterium much more slowly than the other amide NH protons (not shown), as expected for H-bonded amide NH protons. In a perfect α helix, there would also be a hydrogen bond from one of the two amide protons at the C terminus to the carbonyl oxygen atom of Ala2, but the NMR data showed that there were two configurations for this terminal solvent-exposed amide group (Figure 4A).

The three-dimensional structure of **2a** was initially calculated from 44 ROE distance restraints (Table S5, Supporting Information) and three $^3J_{\text{NHCH}\alpha}$ ($\phi = -60 \pm 25^\circ$) coupling constant restraints using a dynamic simulated annealing and energy minimization protocol in XPLOR (version 3.851). The resulting structures (calculated without Pden^{2+}) showed reasonable structural convergence to a helix,

(39) Dyson, H. J.; Cross, K. J.; Houghten, R. A.; Wilson, I. A.; Lerner, R. A. *Nature* **1985**, *318*, 480.

(40) Kessler, H. *Angew. Chem., Int. Ed. Engl.* **1982**, *21*, 512.

(41) (a) Rajashankar, K. R.; Ramakumar, S.; Mal, T. K.; Chauhan, V. S. *Angew. Chem., Int. Ed. Engl.* **1994**, *33*, 970–973. (b) Karle, I. L.; Balaram, P. *Biochemistry* **1990**, *29*, 6747–6756. (c) Wienken, M.; Zangrando, E.; Randaccio, L.; Menzer, S.; Lippert, B. *J. Chem. Soc., Dalton Trans.* **1999**, 459–465.

(37) Williamson, M. P. *Biopolymers* **1990**, *29*, 1423.

(38) Wishart, D. S.; Sykes, B. D.; Richards, F. M. *Biochemistry* **1992**, *31*, 1647.

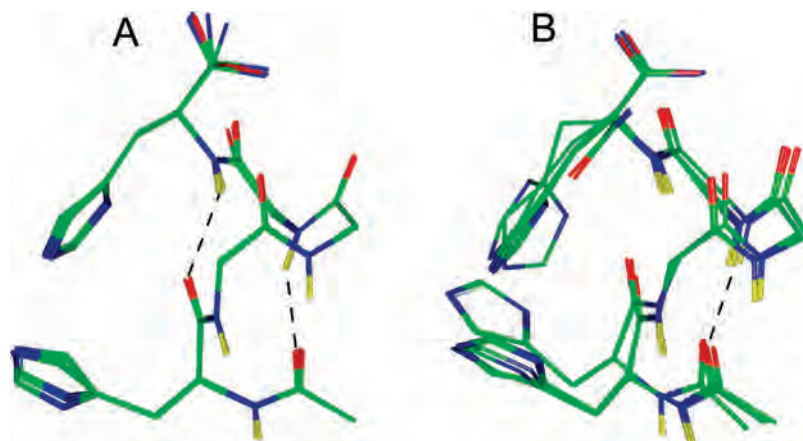


Figure 4. Backbone superimposition of the 14 lowest-energy refined structures of isomer **2a** (Ala-methyls omitted for clarity) in (A) DMF- d_7 , showing more defined structure than in (B) 90% $\text{H}_2\text{O}/10\%$ D_2O . Dashed lines represent hydrogen bonds identified from VT-NMR experiments.

but a number of small ROE violations remained. These violations disappeared when Ala4 and His5 amide NHs were constrained by the $5 \rightarrow 1$ α -helical hydrogen bonds to the acetyl and His1 carbonyl oxygens, respectively, the hydrogen bonds being supported by the VT-NMR data. These two hydrogen bond constraints, which correspond to two of three H bonds expected for an α -helical **2a**, improved structural convergence and markedly reduced the energies of calculated structures. Figure 4a shows a superimposition of the 14 lowest-energy calculated three-dimensional structures for **2a** in a DMF- d_7 solution. This final structure shows an unusually well-defined single turn of an α helix. Ramachandran analysis of the 14 lowest-energy structures showed ϕ (-59° to -71°) and ψ (-31° to -60°) angles typical of an α helix for all residues except for His5, ϕ (-75° to -84°) and ψ (-34° to -164°). This suggests that there is some “fraying” of the helix at the C-terminal end of the peptide, as often observed in short peptide helices due to solvation by water.⁴⁰

The $\text{Pd}(\text{en})^{2+}$ moiety was not included in the structure calculation due to uncertainties with metal force fields. We have so far not been able to successfully produce highly accurate NMR structures using Pd force fields in calculations from this laboratory using available NMR software programs. However, the calculated structure unambiguously locates the positions and orientations of the two imidazole rings and thus also identifies the precise location of the coordinated Pd^{2+} ion. The ^{13}C chemical shift data above also clearly indicate that the N1 atom of each imidazole ring is bound to the metal ion. The calculated structure confirms this assignment. Known histidine complexes of Pd(II) show square-planar geometry around palladium(II),⁴² the N1–Pd–N1 angle being $90 \pm 5^\circ$, which requires the average separation between coordinating N1 atoms to be $\sim 2.7 \text{ \AA}$, corresponding to a Pd–N1 bond length of 1.90 \AA . Our initial peptide structure determination was calculated without an N1 \cdots N1 distance constraint; however, when this constraint was incorporated (final displayed structure, Figure 4), there was better structural convergence (lower rmsd). This is supported by NOE data, which is consistent with a separation between,

and the trajectories of, the imidazoles in a square-planar complex. This is consistent with structures of known histidine complexes of palladium(II) that show square-planar geometry around palladium.⁴²

Structure of $[\text{Pd}(\text{en})(\text{AcHAAAHNH}_2\text{--NI,NI})]^{2+}$ (2a**) in Water.** The corresponding reaction of **1** with $[\text{Pd}(\text{en})(\text{ONO}_2)_2]$ in water (90% $^1\text{H}_2\text{O}$, 10% $^2\text{H}_2\text{O}$) adjusted to pH 5 also produced three species as indicated by ^{15}N NMR (Supporting Information, Figure S3) and ^1H and ^{13}C NMR spectral data (Supporting Information, Table S3). The species can again similarly be assigned to metallopeptides **2a–2c** on the basis of this information.

NOESY spectra were recorded for **2a** in water, and the NOE summary diagram (Figure 2b) shows that the measured parameters (NOEs, $^3J_{\text{HNCH}\alpha}$, and detectable H bonds) are similar to those obtained in DMF (Figure 2a). However, the chemical shifts for the putative hydrogen-bond-forming amide NH protons of His5 and Ala4 in **2a** are not quite as temperature-independent in water as in DMF (Figure S5b, Supporting Information); the $^3J_{\text{HNCH}\alpha}$ coupling constants for **2a** do not differ quite as much from random coil values as do those in DMF (Table S6, Supporting Information), and the chemical shifts for peptide backbone $\text{CH}\alpha$ protons in **2a** do not vary as much from free peptide values in water as they did in DMF (Figure 3b vs a). The ROEs for **2a** in water were slightly less intense than the ROEs for **2a** in DMF, and the final structure calculations generated 14 lowest-energy structures from water (Figure 4b) that do not superimpose as tightly as from DMF (Figure 4a).

Thus, it is clear that, while the pentapeptide **1** does become α -helical in water in the presence of the Pd initiator (Figure 4b), there is a lower proportion of helicity in water than in DMF. This is attributed to the hydrogen-bond donor water molecules (55 M concentration) competing with amide NH protons for the peptide carbonyl oxygens, and thus intermolecular H bonds predominate over helix-defining intramolecular main-chain hydrogen bonds. In DMF, there is only competition from hydrogen-bond-accepting solvent oxygen atoms which appear to have less effect on intramolecular peptide H-bonding partners.

(42) Wienken, M. E. Z.; Randaccio, L.; Menzer, S.; Lippert, B. *J. Chem. Soc., Dalton Trans.* **1993**, 21–24, 3349.

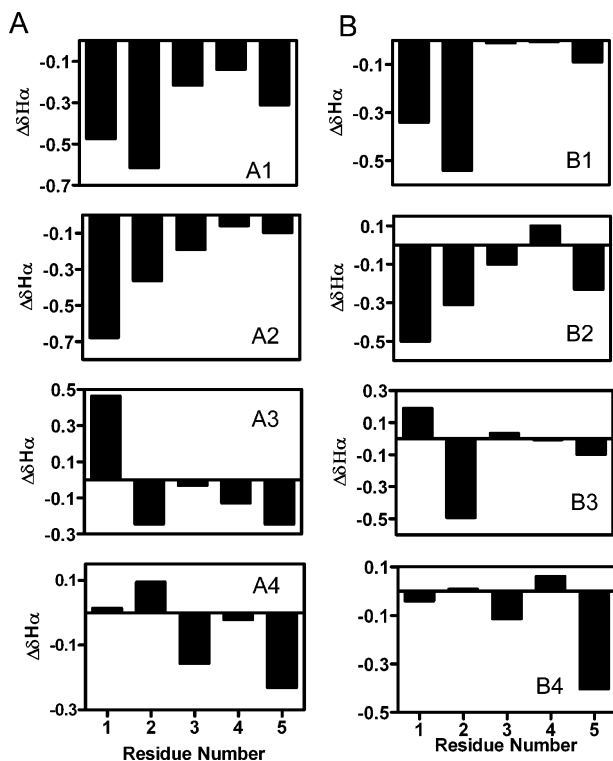


Figure 5. Deviations of CH α chemical shifts in (A1, B1) **7**, (A2, B2) **8**, (A3, B3) **9**, and (A4, B4) **10**, relative to the free peptide **1**, $\Delta\delta = \delta\text{CH}\alpha(\text{complex}) - \delta\text{CH}\alpha(\text{free peptide})$ in (A) DMF- d_7 or (B) 90% H $_2$ O/10% D $_2$ O. Negative values indicate upfield shifts for the metal complex versus free peptide, and more negative than -0.1 ppm is typical of α -helicity.

NMR of N-Methylated Peptides Bound by Pd(en) $^{2+}$.

The ROESY correlations (Table S7, Supporting Information) observed for the complex [Pd(en)(AcH*AAAH* NH_2)] $^{2+}$ (**7**), with two N3-methylated imidazole rings, in both DMF- d_7 and water were very similar to those for **2a**, indicating that an α -helical structure was present. The chemical shifts of the methine H atoms of the amino acid residues (Figure 5), and HNCH coupling constants involving these protons (Table S6, Supporting Information), were similar to those observed for **2a**, again consistent with a helical structure. By contrast, the Pd(en) $^{2+}$ complexes with the three other methylated peptides did not show any long-range ROESY correlations, as expected if there was no strong preference for an α -helical structure in these species. However, it should be noted that there was much overlapping of peaks in the spectra of [Pd(en)(AcH*AAAH* NH_2)] $^{2+}$ (**8**), and it is possible that some correlations were not observed. The ^1H NMR spectrum of **8** in water also showed some broad resonances, notably NH signals for Ala3 and Ala4 and Ala2 CH α and His#5 CH $_3$. These peaks became sharper as the sample was heated, although the Ala2 CH α and Ala3 NH signals remained broad up to 318 K, with pH not affecting broadening. It is likely that the broadening arose from interconversion between different conformations. In DMF- d_7 , all five residues showed negative values ($\Delta\delta\text{H}\alpha$; Figure 5), but the values for Ala4 (-0.05 ppm) and His#5 (-0.09 ppm) were smaller than the -0.1 ppm usually considered a threshold. In water (Figure 5), four residues gave negative values for $\Delta\delta\text{H}\alpha$ (only slightly so for Ala3), but a significant positive value for Ala4.

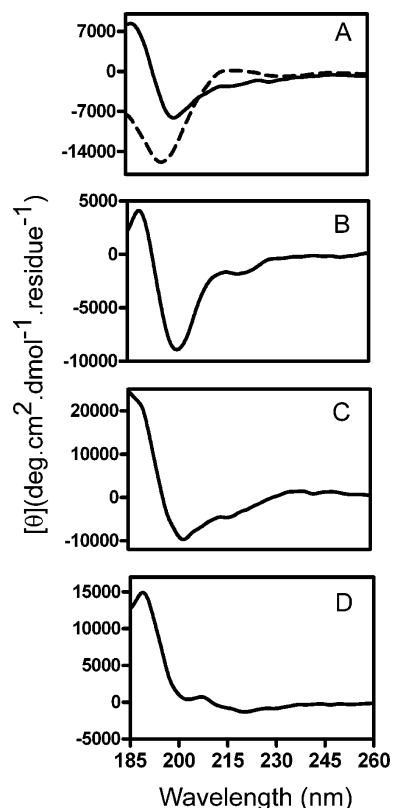


Figure 6. CD spectra change upon the addition of [Pd(en)(ONO $_2$) $_2$] to the free peptide (A) for **1**, (B) for **3**, (C) for **4**, and (D) for **5** forming **2**, **7**, **8**, **9** respectively. Dotted lines, free peptide **1**; solid lines, peptide and [Pd(en)(ONO $_2$) $_2$] at ratio 1:1. CD measurements were performed at 50 μM of the peptide and in a phosphate buffer solution at pH 7.0.

The values of $^3J_{\text{HNCH}\alpha}$ for **8** in DMF- d_7 (Figure 6) were < 6 Hz for His#1, Ala2, and Ala3; slightly > 6 Hz for Ala4; and much greater for His#5. Variable-temperature NMR studies of the NH protons of **8** in water (Figure S6, Supporting Information) showed low-temperature coefficients for the peptide proton of His#5 and terminal NH $_2$, as expected for an α helix, but the peptide proton of Ala4 did not. There was no clear evidence, as there was for **7**, for a predominant helical conformation, but it is possible that there was interconversion between a helical conformation and nonhelical conformation(s).

For [Pd(en)(AcH*AAAH* NH_2)] $^{2+}$ (**9**) in DMF- d_7 or water, there were no long-range ROESY correlations. CH α chemical shifts (Figure 5) and HNCH α coupling constants (Table S6, Supporting Information) were not as expected for a helical conformation. VT-NMR spectra only showed one NH signal with low-temperature coefficients, Ala3 < 4 ppb/K. There was no strong evidence for helicity. [Pd(en)(AcH*AAAH* NH_2)] $^{2+}$ (**10**) in DMF- d_7 showed very broad peptide H signals, as mentioned above, making ROE correlations difficult to identify due to low intensity. A determination of HNCH α coupling constants was not possible, and H α shifts (Figure 5) provided no evidence for helicity.

Circular Dichroism Spectra. A highly α -helical peptide gives a distinctive CD spectrum with a negative band at 222 nm due to the peptide carbonyl n to π^* transition, a negative band at 208 nm, and a positive band at 192 nm from π to π^* transition. In water, each of the free peptides **1**, **3**–**5** showed

a CD spectrum expected for a random coil conformation. For example, the CD spectrum of AcHAAAHNH₂ (**1**) is shown in Figure 6A.

The CD spectrum of [Pd(en)(AcH[#]AAAHNH₂)²⁺] (**7**) is shown in Figure 6B. It shows a small negative band at 219 nm, a large negative band at 200 nm, and a large positive band at 189 nm. The presence of these peaks was indicative of some helicity, but their relatively low intensities indicated that the degree of helicity was not large, with much of the peptide present in a random coil conformation. This agrees with the discussion of the NMR spectra for **7** above, which indicated some helicity in water but less than in DMF.

The CD spectrum of [Pd(en)(AcH[#]AAAHNH₂)²⁺] (**8**) is shown in Figure 6C. It shows negative bands at 218 and 202 nm, and a large positive band at 190 nm. These bands, on face value, are indicative of a helical conformation, and their intensities appear to indicate greater helicity than for **7**. This appears to contradict our interpretation of the NMR data as indicating less helicity for **8** than for **7**—we suggested above a possible interconversion between a helical structure and another conformation. This second conformation would give a CD spectrum similar in some respects to that expected for a helix. Some types of β -turn conformations reportedly show such CD spectra.

The CD spectrum of [Pd(en)(AcH[#]AAAHNH₂)²⁺] (**9**) is shown in Figure 6D. It shows a very small negative band at 221 nm, a small positive band at 207 nm, a small negative band at 202 nm, and a very large positive band at 189 nm. This spectrum is inconsistent with all known major secondary structures, but the large positive band at 189 nm suggests that there was some structure present, and that it was not a random coil.

The CD spectrum of [Pd(en)AcHAAAHNH₂]²⁺ (**2**) is shown in Figure 6A. Since we know that there are three linkage isomers, **2a–2c**, corresponding to **7–9**, respectively, it is not surprising that this spectrum can be reproduced by adding the spectra of **7–9** weighted by the known populations of the three isomers in **2**.

Other Metal Ions and Solvents. Both peptide **1** and [Pd(en)(ONO₂)₂] dissolved readily in dimethylsulfoxide, but this solvent coordinates strongly to palladium and was not useful for our studies. The addition of equimolar ZnCl₂ or Zn(CF₃SO₃)₂ to Ac-HAAAHNH₂ in DMF-*d*⁷ gave a solution with broad ¹H NMR peaks, attributed to the formation of labile zinc complexes and a facile migration of Zn²⁺ ions between coordination sites. Even for peptide **3** with two (N3-MeHis) residues (where only one linkage isomer would be present), peaks were broad. The reaction of ¹⁵N-labeled [Pt(en)(ONO₂)₂] with Ac-HAAAHNH₂ (**1**) in DMF was very slow; peaks that eventually appeared did not correspond to complexes with a large chelate ring and metal bound by nitrogens of two imidazoles. Instead, ¹⁵N NMR spectra suggested that the metal was coordinated by the N3 of each imidazole, with the formation of a six-membered chelate ring involving the adjacent peptide nitrogen, as previously observed for other metalloptides. Pentapeptide **3** with two (N3-MeHis) residues, having more restricted coordination sites, still gave a slow reaction with *cis*-[Pt(¹⁵NH₃)₂(ONO₂)₂]

in DMF, and a multitude of peaks were observed in the ¹⁵N NMR spectrum.

Discussion

This work¹ unequivocally demonstrates that a pentapeptide with histidine residues at *i* and *i* + 4 binds to Pd²⁺ with two coordination sites available to form a macrochelate ring. For metal coordination to two imidazoles in the pentapeptide Ac-HAAAHNH₂, there are four possible linkage isomers (N1,N1), (N1,N3), (N3,N1), and (N3,N3). The first three of these are all observed, with 22-, 21-, and 21-membered rings, respectively. The fourth, with N3,N3 coordination, forms a 20-membered ring that is likely more strained, and this linkage isomer is not observed. To confirm the possibility of forming the 20-membered (N3,N3) isomer, we did react the N1-methyl,N1-methyl peptide and isolated the complex, showing that its formation from Ac-HAAAHNH₂ must be thermodynamically nonpreferred when competing with N1,N1 and N1,N3 and N3N1. Usually, metal ions tend to favor five- and six-membered metallocyclic rings in small inorganic compounds. However, in this case, the much larger 21- and 22-membered metallocycles that are formed here are quite stable. There was no detectable free peptide in solution (water or DMF) after the addition of just 1 equiv of the palladium complex. Over several days, depending upon the amount of water present, appreciable NH₄⁺ signals began to appear in the proton NMR spectrum (Figure S7, Supporting Information) suggesting some slow palladium-mediated hydrolysis (50% after 7 days) at the C-terminal amide bond (Ac-HAAAHNH₂ → Ac-HAAAHOH + NH₄⁺).

Peptides as small as this do not normally form an α helix. Usually, > 15 peptide residues are necessary to form enough intramolecular hydrogen bonds to achieve thermodynamic stability for an α -helical peptide conformation. Yet, we have shown here that Pd(en)²⁺ acts as a “metal clip” that enables the N1,N1 linkage isomer to adopt an α -helical conformation. This is favored over other conformations, such as the random coil, that are also observed to some extent in DMF, and to a larger extent in water. We observe only two intramolecular hydrogen bonds in the stable helical structures observed herein for a pentapeptide. It would thus appear that metal chelation via two appropriately spaced histidine imidazoles can overcome the thermodynamic barrier to the formation of an α -helical turn, suggesting that metalloptides of this or greater length must have largely kinetic or entropic barriers to the formation of α -helical structures. Competition by the protic solvent water for the hydrogen-bonding peptide amides, which otherwise form intramolecular H bonds that define helicity, accounts for reduced helicity in water compared with the aprotic solvent DMF. The side-chain imidazoles have a high intrinsic affinity for metal ions, with each of the two imidazole nitrogens having comparable affinity. Their highly constrained nature may also assist in sufficiently separating the α carbons of His1 and His5 to avoid the formation of smaller β or γ turns in the peptide and encourage the formation of the larger α turn that defines an α helix (Figure 7). Metal coordination to histidine side chains can be readily reversed (e.g., by adding thiourea),

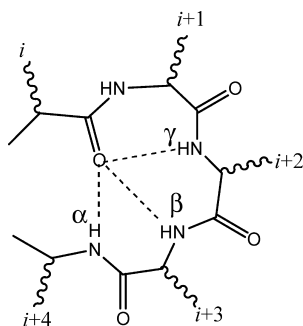


Figure 7. Putative hydrogen bonds that distinguish α , β , and γ turns in a peptide.

suggesting the possibility of using such removable metal clips to aid the folding of polypeptides and proteins. This facile coordination and removal of the helix-inducing agent contrasts with the irreversible nature of covalent organic linkers⁶ or caps⁷ used to potentially stabilize α helicity in a peptide and with high molecular weight folding agents such as protein chaperones.

The examples of $[\text{Pd}(\text{en})(\text{AcH}^*\text{AAAH}^*\text{NH}_2)]^{2+}$ (**8**) and linkage isomer **2b** of $[\text{Pd}(\text{en})(\beta\text{HAAAHHNH}_2)]^{2+}$, where the CD spectrum on face value suggests a high degree of helicity that is clearly refuted by NMR data, demonstrate the danger of using CD spectra alone as an indicator of peptide conformation without additional supporting information derived from other techniques. The observation that, of the possible linkage isomers, only N1,N1 coordination enforced in the His*,His* peptide with N3 methylation has substantial α helicity justifies our decision to use N3-methylated histidine residues (His*) in our work with thermolysin mimics and other peptides. Clearly, studies of metal binding to peptides containing histidine are compromised by the issue of linkage isomerism and the likelihood of formation of multiple linkage isomers with different peptide conformations. Even for the one linkage isomer shown here to induce α helicity, the

relatively low degree of induced helicity in water indicates that there is still an opportunity to further optimize α -helix induction in metalloptides.

To form large stable chelate rings of the type reported herein, it is also likely that the metal ion needs to fall into a certain window of lability. A relatively inert metal ion like Pt^{2+} tends to become trapped in local energy minima, represented by small chelate rings involving coordination to imidazole-N3 and to amide atoms of the peptide backbone. The more labile Pd^{2+} is able to fall more easily into the overall energy minimum represented by the very large chelate ring spanning both imidazole rings. However, palladium complexes are not so labile that the ethylenediamine ligand is easily lost, so that coordination by the peptide is limited to two adjacent coordination sites, and the lifetime for each individual isomer is sufficiently long for it to be characterized in solution by NMR spectroscopy. On the other hand, Zn^{2+} is likely to be too labile to allow individual isomers of short peptides to be characterized, despite the prevalence of zinc–histidine linkages in larger zinc finger proteins.²⁰ Metal ions other than Pd^{2+} that may also fit this window of lability (e.g., Ru^{2+}), metal binding groups other than the imidazole rings of histidine residues, and different spacings between the metal-binding sites in peptides need to be investigated for their capacity to form metalocycles that can induce structure in peptides of biological interest.

Supporting Information Available: 1D and 2D proton, carbon, and nitrogen NMR spectra; mass spectra; VT-NMR plots (seven figures); and spectral data such as chemical shifts, coupling constants, and NOE correlations (seven tables; 23 pages). This material is available free of charge via the Internet at <http://pubs.acs.org>.

Acknowledgment. We thank the Australian Research Council for research support and for a Federation Fellowship (D.P.F.).

IC800970P